Impact of oxygen plasma postoxidation process on Al2O 3 / n -In0.53Ga0.47As metal-oxide-semiconductor capacitors

Y. Lechaux, A. Fadjie-Djomkam, S. Bollaert, Nicolas Wichmann

Applied Physics Letters

Impact of oxygen plasma postoxidation process on Al_2O_3/*n*-$In_{0.53}Ga_{0.47}As$ metal-oxide-semiconductor capacitors

Cite as: Appl. Phys. Lett. **109**, 131602 (2016); https://doi.org/10.1063/1.4963656
Submitted: 08 July 2016 • Accepted: 14 September 2016 • Published Online: 27 September 2016

Y. Lechaux, A. B. Fadjie-Djomkam, S. Bollaert, et al.

Impact of oxygen plasma postoxidation process on Al_2O_3/*n*-$In_{0.53}Ga_{0.47}As$ metal-oxide-semiconductor capacitors

Y. Lechaux, A. B. Fadjie-Djomkam, S. Bollaert, and N. Wichmann
Institute of Electronics, Microelectronics and Nanotechnology, University of Lille 1, CNRS UMR 8520, Avenue Henri Poincaré, 59652 Villeneuve d'Ascq, France

(Received 8 July 2016; accepted 14 September 2016; published online 27 September 2016)

Capacitance-voltage (C-V) measurements and x-ray photoelectron spectroscopy (XPS) analysis were performed in order to investigate the effect of a oxygen (O_2) plasma after oxide deposition on the Al_2O_3/*n*-$In_{0.53}Ga_{0.47}As$ metal-oxide-semiconductor structure passivated with ammonia NH_4OH solution. From C-V measurements, an improvement of charge control is observed using the O_2 plasma postoxidation process on $In_{0.53}Ga_{0.47}As$, while the minimum of interface trap density remains at a good value lower than 1×10^{12} cm^{-2} eV^{-1}. From XPS measurements, we found that NH_4OH passivation removes drastically the Ga and As native oxides on the $In_{0.53}Ga_{0.47}As$ surface and the O_2 plasma postoxidation process enables the reduction of interface re-oxidation after post deposition annealing (PDA) of the oxide. The advanced hypothesis is the formation of interfacial barrier between Al_2O_3 and $In_{0.53}Ga_{0.47}As$ which prevents the diffusion of oxygen species into the semiconductor surface during PDA. *Published by AIP Publishing.*
[http://dx.doi.org/10.1063/1.4963656]

III–V low bandgap compound semiconductors such as InAs, GaSb, or $In_{0.53}Ga_{0.47}As$ are promising materials for high-frequencies performance metal-oxide-semiconductor field effect transistors (MOSFETs) due to their high electrons mobility[1–3] and their bandgap engineering possibilities. However, compared to silicon with the SiO_2-Si gate stack which leads to low value of interface trap density (D_{it}), the oxide and interface quality between oxide and III–V semiconductor with low D_{it} is still a challenge to avoid strong Fermi-level pinning[4] and deterioration of channel mobility. It has been reported that high D_{it} value on the Al_2O_3/$In_{0.53}Ga_{0.47}As$ interface is attributed to Ga dangling bonds, As dimers, or III–V natives oxides.[5–7] However, pretreatments such as ammonium hydroxide[8] and ammonium sulfide passivations,[9–12] hydrogen[13] or nitrogen plasma,[14] and using interfacial AlN layer[15] or nitridation treatment[16] lead to a shift or a reduction of midgap D_{it}. In fact, low values of D_{it} in the range of 1×10^{12} cm^{-2} eV^{-1} have been demonstrated on the $In_{0.53}Ga_{0.47}As$ MOS systems using different treatments and different gate oxides such as Al_2O_3,[17,18] HfO_2,[19] ZrO_2,[2] and BeO.[20] Previous works from Takagi *et al.* on Al_2O_3/Ge gate stack using enhanced resonance cyclotron oxygen plasma report on the reduction of interface trap density by creating interfacial layer.[21,22] In this letter, we proposed to further improve electrical and interfacial properties of Al_2O_3–$In_{0.53}Ga_{0.47}As$ interface using *in-situ* O_2 plasma postoxidation process in atomic layer deposition (ALD) chamber.

In this work, metal-oxide-semiconductor capacitors (MOSCAPs) were fabricated and electrically characterized. Epitaxial layer was grown by solid source molecular beam epitaxy (MBE) on the InP substrate (100). It was composed as follows: an $Al_{0.52}In_{0.48}As$ buffer layer, a highly Si-doped (1×10^{19} cm^{-3}) *n*-type $In_{0.53}Ga_{0.47}As$ layer for ohmic contact, and a Si-doped (2×10^{16} cm^{-3}) *n*-type $In_{0.53}Ga_{0.47}As$ top layer. Prior to the ALD deposition, the $In_{0.53}Ga_{0.47}As$ surface was degreased in acetone, isopropanol, and rinsed in deionized water (DIW). Then, a surface treatment was used in order to eliminate native oxides and passivate the $In_{0.53}Ga_{0.47}As$ surface. Thus, sample was immersed in 4% diluted NH_4OH solution for 10 min followed by immersion in DIW. 2 nm of Al_2O_3 was deposited by ALD at 250 °C from trimethylaluminium (TMA) and water (H_2O) precursors followed by *in-situ* O_2 plasma postoxidation process. The O_2 plasma postoxidation process consists of remote plasma with 100 W radiofrequency source using O_2 (100 sccm) and Ar (200 sccm) in the ALD chamber at 250 °C. A metal grid between the substrate and plasma source is used to prevent ion bombardment and thus only radicals reach the substrate. For higher thickness, diffusion of oxygen species should be limited and it could prevent formation of interfacial layer and then increase the interface trap density as observed by Zhang *et al.*[21] Then, 2 nm of ALD-Al_2O_3 was added to obtain a total oxide thickness of 4 nm. A post-deposition annealing (PDA) at 600 °C under forming gas (N_2H_2) was performed to stabilize the oxide. Circular Ni/Au top gate contacts were subsequently evaporated. After etching of low doped *n*-type $In_{0.53}Ga_{0.47}As$ layer by wet etching process, source contacts were deposited by evaporation of Ti/Pt/Au on the highly Si-doped (1×10^{19} cm^{-3}) *n*-type $In_{0.53}Ga_{0.47}As$ layer to form ohmic contact. Reference sample without the O_2 plasma postoxidation process was also fabricated with 4 nm Al_2O_3 deposited by ALD and transmission electron microscopy confirmed equal thickness of both samples.

C-V measurements were carried out in order to characterize the electrical properties of the Al_2O_3–$In_{0.53}Ga_{0.47}As$ interface on MOSCAPs. Measured capacitance and conductance were extracted using Agilent 4294A precision impedance analyzer in the frequency range from 100 Hz to 1 MHz at room temperature. Figure 1 shows the C-V characteristics as a function of gate-source voltage (V_{gs}) for samples without

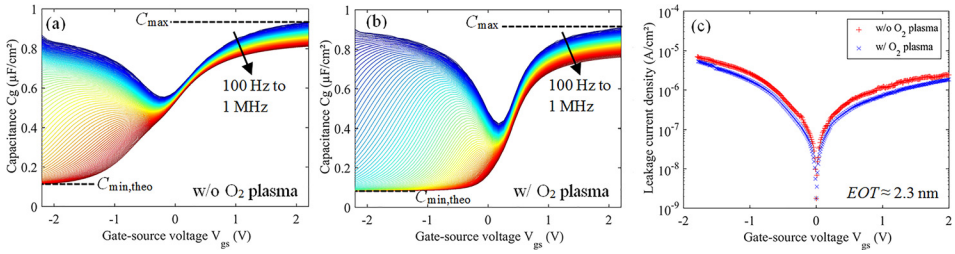

FIG. 1. C-V characteristics at room temperature of Al_2O_3/n-InGaAs MOSCAPs (a) without and (b) with the O_2 plasma postoxidation process and (c) leakage current density as a function of gate-source voltage for both samples.

(Fig. 1(a)) and with (Fig. 1(b)) O_2 plasma postoxidation process. First, in depletion region (between $V_{gs} = -0.5$ V and $V_{gs} = 0.5$ V), the C-V stretch-out is considerably reduced and minimum capacitance at low frequency is lower for the sample with O_2 plasma treatment. Moreover, the minimum inversion capacitance (C_{min}) observed at high frequency is also lower for this sample ($C_{min} = 0.08\ \mu F/cm^2$) and is close to the theoretical value for a 2×10^{16} cm^{-3} *n*-type $In_{0.53}Ga_{0.47}As$ MOSCAPs ($C_{min,theo} = 0.06\ \mu F/cm^2$). The humps observed in the inversion region that start at higher frequency for the sample with O_2 plasma process suggested a reduction of interface traps density. Such humps were also observed by Krylov *et al.* comparing Si_3N_4 and Al_2O_3 gate oxides[8,23] and were attributed to false inversion due to the midgap interface states.[24,25] The previous observations suggest an improvement of Fermi level movement (Fermi level unpinning) at the interface and lower D_{it} for the sample treated with O_2 plasma postoxidation process. However, the maximum accumulation capacitance ($C_{max} \approx 0.9\ \mu F/cm^2$) for both samples is lower than oxide capacitance (C_{ox}) estimated at $1.44\ \mu F/cm^2$. This effect can be related to the low density of state of the $In_{0.53}Ga_{0.47}As$ conduction band which considerably reduces the accumulation capacitance. Besides, as maximum accumulation capacitances at 1 kHz are equal for both samples, the effective oxide thickness ($EOT \approx 2.3$ nm) is not modified using the O_2 plasma treatment. Furthermore, we observed for both samples a large frequency dispersion in accumulation region, between $V_{gs} = 1$ V and $V_{gs} = 2$ V. This dispersion in accumulation is not clear and is likely attributed to border traps in oxide close to interface.[26,27] In order to estimate the current leakage, current-voltage (I-V) measurements were performed (Fig. 1(c)). A value of 1×10^{-5} A cm^{-2} was obtained for both samples indicating a good oxide quality. Moreover, a slight reduction of leakage current is observed using the O_2 plasma treatment.

Interface trap density was evaluated by means of conductance method developed by Nicollian and Brews.[28] From the measured conductance, normalized parallel conductance $[(Gp/\omega)/Aq]$ was calculated[28] where Gp is the equivalent parallel conductance, ω is the angular frequency, A is the surface area of top gate contact, and q is the elementary charge. Figure 2 shows the normalized parallel conductance map without (Fig. 2(a)) and with O_2 plasma postoxidation process (Fig. 2(b)). This map shows the magnitude of the normalized parallel conductance $[(Gp/\omega)/Aq]$ as a function of frequency and V_{gs} at RT. The frequency shift with gate voltage of $[(Gp/\omega)/Aq]_{max}$ is an indicator of Fermi level movement at $Al_2O_3/In_{0.53}Ga_{0.47}As$ interface. If $[(Gp/\omega)/Aq]_{max}$ is moving vertically with gate bias, the band bending is efficient.[24,29] Therefore, as indicated in Fig. 2(b), Fermi level movement is improved with the O_2 plasma postoxidation process. Moreover, $[(Gp/\omega)/Aq]_{max}$ does not move for frequencies less than 20 kHz (Fig. 2(a)) and 600 Hz (Fig. 2(b)) suggesting that Fermi level can be moved for lower energies into bandgap with the O_2 plasma process.[29] Both samples show D_{it} lower than $1 \times 10^{12}\ cm^{-2}\ eV^{-1}$. Astonishingly, we noticed a lower value for sample without O_2 plasma process ($D_{it} = 6 \times 10^{11}\ cm^{-2}\ eV^{-1}$) compared to the sample with O_2 plasma ($D_{it} = 8 \times 10^{11}\ cm^{-2}\ eV^{-1}$) which is probably due to large frequency dispersion observed in accumulation region.

XPS measurements were performed in order to characterize the Al_2O_3/n-type $In_{0.53}Ga_{0.47}As$ interface. An Al $K\alpha$ radiation ($h\upsilon = 1486.6$ eV) was used as an excitation source and the measurements were obtained at a pressure of 5×10^{-9} mbar at 75° angle. First, we analyzed the effect of NH_4OH passivation. Figure 3 shows the XPS spectra of In $3d_{5/2}$, Ga $2p_{3/2}$ and As $2p_{3/2}$ (top) without passivation and (bottom) with NH_4OH passivation. For each component, we noticed the presence of native oxides at higher binding energy with respect to the bulk core-levels (ΔBE) which is reduced using NH_4OH passivation. For In 3*d* core-levels (Figs. 3(a) and 3(d)), native In-O (ΔBE = +1 eV) is decreased of about 10% of total area with a shift to lower binding energy (ΔBE = +0.6 eV) after the NH_4OH passivation. Same effects were observed on Ga 2p core-levels (Figs. 3(b) and 3(e)) where native Ga-O (ΔBE = +1.2 eV) is decreased of about 34% of total area with a shift to lower binding energy (ΔBE = +0.8 eV) after NH_4OH passivation suggesting a modification of both In-O and Ga-O stoichiometry. For As 2p core-levels (Figs. 3(c) and 3(f)), we noticed two native oxides before passivation, As_2O_3 and As_2O_5 (ΔBE = +3.3 eV and ΔBE = +4.4 eV, respectively). However after passivation, As_2O_5 oxide is found to be below the detection threshold whereas area of As_2O_3 component slightly decreases without a significant shift of its binding energy.

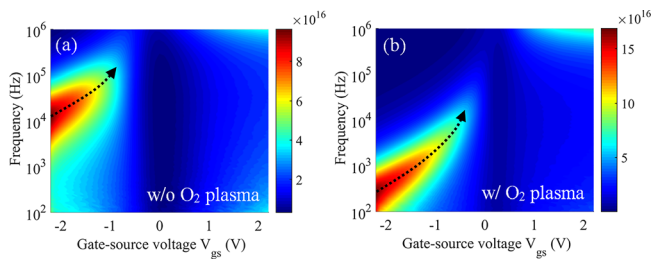

FIG. 2. Conductance map representing magnitude of the normalized parallel conductance as a function of frequency and gate voltage of Al_2O_3/n-type $In_{0.53}Ga_{0.47}As$ MOSCAPs (a) without and (b) with the O_2 plasma postoxidation process. The dotted-line arrow is a guide to the eye to trace the position of the normalized parallel conductance maximum.

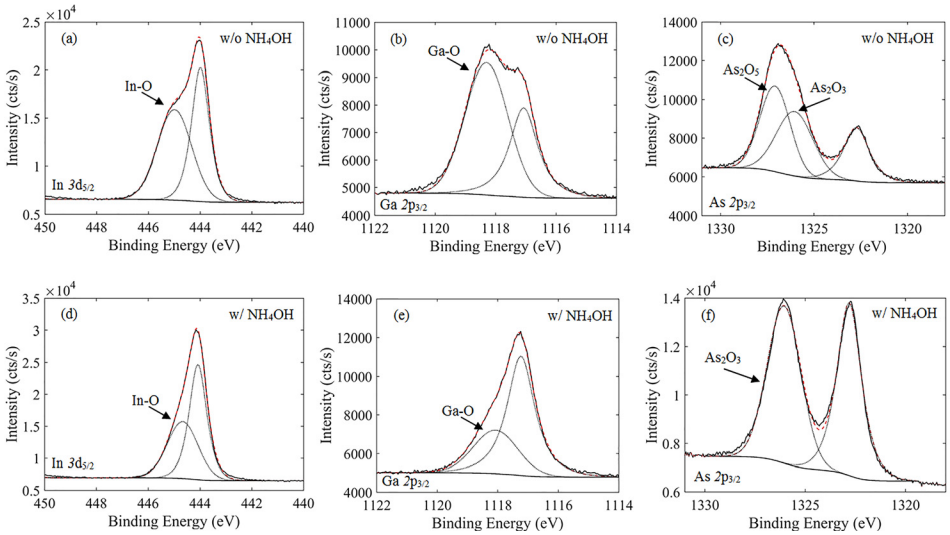

FIG. 3. XPS Spectra of *n*-type $In_{0.53}Ga_{0.47}As$ surface (top) without passivation and (bottom) with NH_4OH passivation (bottom). (a)–(d) For In $3d_{5/2}$ core-levels, (b)–(e) for Ga $2p_{3/2}$ core–level, and (c)–(f) for As $2p3/2$ core-levels.

Second, we focused on the In $3d_{5/2}$ XPS spectra to study the effect of O_2 plasma postoxidation process. Figure 4 shows the XPS spectra of In $3d_{5/2}$ after NH_4OH passivation, Al_2O_3 deposition, and post deposition annealing for the samples (Fig. 4(a)) without and (Fig. 4(b)) with the O_2 plasma postoxidation process. Compared with Fig. 3(d), In-O is shifted to higher binding energy ($\Delta BE = +1.8$ eV) for samples with or without the O_2 plasma process, indicating a modification of In-O stoichiometry. Furthermore, for the sample without treatment an increase in the In-O peak area[30] of about 6% of total area is observed compared to the sample with O_2 plasma. Thus, the O_2 plasma postoxidation process prevents the diffusion of oxygen species into the semiconductor surface during post deposition annealing and limits the interface re-oxidation. The hypothesis we proposed is the creation of an interfacial layer between InGaAs and Al_2O_3 as observed by Takagi and coworkers with Al_2O_3/Ge gate stacks.[22]

In summary, we have demonstrated the improvement of Fermi level movement efficiency on Al_2O_3/*n*-type $In_{0.53}Ga_{0.47}As$ MOSCAPs using the O_2 plasma postoxidation process. It is found that the O_2 plasma prevents the interface re-oxidation by limiting diffusion of oxygen species from oxide into semiconductor surface. This method yields to Al_2O_3/*n*-type $In_{0.53}Ga_{0.47}As$ MOS capacitors with good electrical properties with D_{it} lower than 1×10^{12} cm^{-2} eV^{-1}. As a result, the oxygen plasma postoxidation method is a promising solution for fabricating gate stacks with good interface quality between oxide and semiconductor for MOSFETs application. Currently, HfO_2-based gate stacks using the O_2 plasma postoxidation process is being investigated.

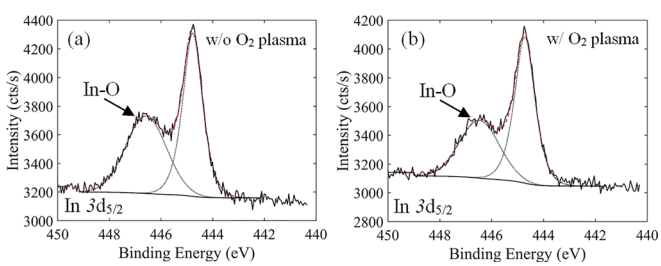

FIG. 4. In $3d_{5/2}$ spectra of *n*-type $In_{0.53}Ga_{0.47}As$ surface after NH_4OH passivation, Al_2O_3 deposition, and post deposition annealing for samples (a) without and (b) with the O_2 plasma postoxidation process.

This work has been supported by the Agence Nationale de la Recherche through the Project No. ANR-13-JS03-0001-01. This work was developed in IEMN's cleanroom, a part of the French National Fabrication Network (RENATECH).

[1]Y. Xuan, Y. Q. Wu, H. C. Lin, T. Shen, and P. D. Ye, IEEE Electron Device Lett. **28**, 935 (2007).
[2]N. Goel, D. Heh, S. Koveshnikov, I. Ok, S. Oktyabrsky, V. Tokranov, R. Kambhampatic, M. Yakimov, Y. Sun, P. Pianetta, C. K. Gaspe, M. B. Santos, J. Lee, S. Datta, P. Majhi, and W. Tsai, Tech. Dig. - IEEE Int. Electron Devices Meet. **2008**, 1–4.
[3]T. D. Lin, W. H. Chang, R. L. Chu, Y. C. Chang, Y. H. Chang, M. Y. Lee, P. F. Hong, M.-C. Chen, J. Kwo, and M. Hong, Appl. Phys. Lett. **103**, 253509 (2013).
[4]K. Martens, W. Wang, K. De Keersmaecker, G. Borghs, G. Groeseneken, and H. Maes, Microelectron. Eng. **84**, 2146 (2007).
[5]J. Robertson, Y. Guo, and L. Lin, J. Appl. Phys. **117**, 112806 (2015).
[6]L. Lin and J. Robertson, Appl. Phys. Lett. **98**, 082903 (2011).
[7]J. Robertson, Appl. Phys. Lett. **94**, 152104 (2009).
[8]I. Krylov, A. Gavrilov, M. Eizenberg, and D. Ritter, Appl. Phys. Lett. **101**, 063504 (2012).
[9]H. D. Trinh, E. Y. Chang, P. W. Wu, Y. Y. Wong, C. T. Chang, Y. F. Hsieh, C. C. Yu, H. Q. Nguyen, Y. C. Lin, K. L. Lin, and M. K. Hudait, Appl. Phys. Lett. **97**, 42903 (2010).
[10]E. O'Connor, B. Brennan, V. Djara, K. Cherkaoui, S. Monaghan, S. B. Newcomb, R. Contreras, M. Milojevic, G. Hughes, M. E. Pemble, R. M. Wallace, and P. K. Hurley, J. Appl. Phys. **109**, 24101 (2011).
[11]M. F. Mohd Razip Wee, A. Dehzangi, S. Bollaert, B. Yeop Majlis, and N. Wichmann, Micro Nano Lett. **8**, 836 (2013).
[12]P. K. Hurley, E. O'Connor, V. Djara, S. Monaghan, I. M. Povey, R. D. Long, B. Sheehan, J. Lin, P. C. McIntyre, B. Brennan, R. M. Wallace, M. E. Pemble, and K. Cherkaou, IEEE Trans. Device Mater. Rel. **13**, 429 (2013).
[13]A. D. Carter, W. J. Mitchell, B. J. Thibeault, J. J. M. Law, and M. J. W. Rodwell, Appl. Phys. Express **4**, 91102 (2011).
[14]V. Chobpattana, J. Son, J. J. M. Law, R. Engel-Herbert, C.-Y. Huang, and S. Stemmer, Appl. Phys. Lett. **102**, 22907 (2013).
[15]Q. H. Luc, E. Y. Chang, H. D. Trinh, Y. C. Lin, H. Q. Nguyen, Y. Y. Wong, H. B. Do, S. Salahuddin, and C. C. Hu, IEEE Trans. Electron Devices **61**, 2774 (2014).
[16]T. Hoshii, S. Lee, R. Suzuki, N. Taoka, M. Yokoyama, H. Yamada, M. Hata, T. Yasuda, M. Takenaka, and S. Takagi, J. Appl. Phys. **112**, 73702 (2012).
[17]J. Hu and H.-S. Philip Wong, J. Appl. Phys. **111**, 44105 (2012).

[18]H.-C. Lin, W.-E. Wang, G. Brammertz, M. Meuris, and M. Heyns, Microelectron. Eng. **86**, 1554 (2009).
[19]Y. Xuan, Y. Q. Wu, T. Shen, T. Yang, and P. D. Ye, Tech. Dig. - IEEE Int. Electron Devices Meet. **2007**, 637–640.
[20]H. S. Shin, J. H. Yum, D. W. Johnson, H. R. Harris, T. W. Hudnall, J. Oh, P. Kirsch, W.-E. Wang, C. W. Bielawski, S. K. Banerjee, J. C. Lee, and H. D. Lee, Appl. Phys. Lett. **103**, 223504 (2013).
[21]R. Zhang, T. Iwasaki, N. Taoka, M. Takenaka, and S. Takagi, Microelectron. Eng. **88**, 1533 (2011).
[22]R. Zhang, T. Iwasaki, N. Taoka, M. Takenaka, and S. Takagi, Appl. Phys. Lett. **98**, 112902 (2011).
[23]I. Krylov, A. Gavrilov, D. Ritter, and M. Eizenberg, Appl. Phys. Lett. **99**, 203504 (2011).
[24]R. Engel-Herbert, Y. Hwang, and S. Stemmer, J. Appl. Phys. **108**, 124101 (2010).
[25]T. Kent, K. Tang, V. Chobpattana, M. A. Negara, M. Edmonds, W. Mitchell, B. Sahu, R. Galatage, R. Droopad, P. McIntyre, and A. C. Kummel, J. Chem. Phys. **143**, 164711 (2015).
[26]E. J. Kim, L. Wang, P. M. Asbeck, K. C. Saraswat, and P. C. McIntyre, Appl. Phys. Lett. **96**, 12906 (2010).
[27]Y. Yuan, L. Wang, B. Yu, B. Shin, J. Ahn, P. C. McIntyre, P. M. Asbeck, M. J. W. Rodwell, and Y. Taur, IEEE Electron Device Lett. **32**, 485 (2011).
[28]E. H. Nicollian and J. R. Brews, *MOS (Metal Oxide Semiconductor) Physics and Technology* (Wiley, New York, 1982).
[29]H. C. Lin, G. Brammertz, K. Martens, G. de Valicourt, L. Negre, W.-E. Wang, W. Tsai, M. Meuris, and M. Heyns, Appl. Phys. Lett. **94**, 153508 (2009).
[30]R. V. Galatage, H. Dong, D. M. Zhernokletov, B. Brennan, C. L. Hinkle, R. M. Wallace, and E. M. Vogel, Appl. Phys. Lett. **99**, 172901 (2011).